Steel and Composite Structures, Vol.14, No. 3 (2013) 205-227
DOI: http://dx.doi.org/10.12989/scs.2013.14.3.205

Flexural-torsional buckling tests of cold-formed steel compression members at elevated temperatures

Yasintha Bandula Heva and Mahen Mahendran*

Faculty of Built Environment and Engineering, Queensland University of Technology, Brisbane, Australia

(Received August 10, 2010, Revised February 01, 2012, Accepted May 17, 2012)

Abstract. Current design standards do not provide adequate guidelines for the fire design of cold-formed steel compression members subject to flexural-torsional buckling. Eurocode 3 Part 1.2 (2005) recommends the same fire design guidelines for both hot-rolled and cold-formed steel compression members subject to flexural-torsional buckling although considerable behavioural differences exist between cold-formed and hot-rolled steel members. Past research has recommended the use of ambient temperature cold-formed steel design rules for the fire design of cold-formed steel compression members provided appropriately reduced mechanical properties are used at elevated temperatures. To assess the accuracy of flexural-torsional buckling design rules in both ambient temperature cold-formed steel design and fire design standards, an experimental study of slender cold-formed steel compression members was undertaken at both ambient and elevated temperatures. This paper presents the details of this experimental study, its results, and their comparison with the predictions from the current design rules. It was found that the current ambient temperature design rules are conservative while the fire design rules are overly conservative. Suitable recommendations have been made in relation to the currently available design rules for flexural-torsional buckling including methods of improvement. Most importantly, this paper has addressed the lack of experimental results for slender cold-formed steel columns at elevated temperatures.

Keywords: cold-formed steel columns; flexural-torsional buckling; column tests; elevated temperatures; fire design

1. Introduction

Slender cold-formed steel columns are generally subject to flexural and/or flexural-torsional buckling modes. Cold-formed steel design standards provide suitable guidelines for columns subject to flexural and flexural-torsional buckling modes at ambient temperature. In recent times, fire performance of cold-formed steel structures has received greater attention due to their increased usage and associated fire threat. Fire performance of slender hot-rolled steel columns has been adequately investigated experimentally (Ali and O'Conner 2001, Wang and Davies 2003a,b, Yang *et al.* 2006) and numerically (Burgress *et al.*1992, Franssen *et al.* 1995,1996, Talamona *et al.* 1997). Further, Eurocode 3 Part 1.2 (ECS 2005) and BS 5950 Part 8 (BSI 1990) provide fire design guidelines for hot-rolled steel compression members. However, there are no specific design guidelines for cold-formed steel compression members at elevated temperature conditions.

*Corresponding author, Professor, E-mail: m.mahendran@qut.edu.au

Eurocode 3 Part 1.2 (ECS 2005) recommends the same fire design guidelines for both hot-rolled and cold-formed steel members, which were originally developed for Class 1, 2 and 3 sections representing hot-rolled steel sections. However, the high section factor of mostly Class 4 cold-formed thin-walled steel sections and the high thermal conductivity of steel lead to rapid steel temperature rise during fires and hence result in lower fire resistance. Therefore the structural behaviour of cold-formed steel structures under fire conditions has emerged as an important area of research in order to improve their fire safety. In recent times, considerable progress has been made in this field by Feng *et al.* (2003a,b,c, 2004), Ranby (1998), Ranawaka and Mahendran (2009a,b,c) and Chen and Young (2007a,b) on local, distortional and flexural buckling of cold-formed steel columns and mechanical properties at elevated temperatures. Many of them have shown that ambient temperature design rules can be used to predict the strengths of cold-formed steel columns at elevated temperatures provided appropriately reduced mechanical properties are used. Their research results provided a strong base for the fire safety research and design of light gauge cold-formed steel structures. However, there have not been any experimental studies on slender cold-formed steel columns at elevated temperatures.

Cold-formed steel design codes, AS/NZS 4600 (SA 2005), Eurocode 3 Part 1.3 (ECS 2006), BS 5950 Part 5 (BSI 1998), the North American Specification (NAS) (AISI 2007), and the Direct Strength Method (DSM) provide suitable design guidelines for cold-formed steel columns subject to flexural-torsional buckling at ambient temperature. Since the member capacity prediction methods used in the current steel design standards are not identical, it is important that their suitability is investigated for the fire design of cold-formed steel compression members.

In practical applications, cold-formed steel columns are likely to be protected by fire resistant materials, resulting in them being subject to a non-uniform temperature distribution. However, if the maximum temperature in the columns can be estimated for a fire event, the column strength under fire conditions can be estimated conservatively using a uniform elevated temperature design method. Hence past research has used this simpler uniform elevated temperature approach (Ranby 1998, Feng *et al.* 2003a,b, Ranawaka and Mahendran 2009b,c).

This paper describes an experimental investigation on the flexural-torsional buckling behaviour of cold-formed steel columns at ambient and elevated temperatures. It considered only the uniform elevated temperature conditions as the aims of this research were to understand the flexural-torsional buckling behaviour at uniform elevated temperatures and to investigate the suitability of both ambient temperature cold-formed steel design and fire design methods. The ambient temperature design methods were modified by including the reduced mechanical properties at elevated temperatures and their accuracy was investigated by using the test results. For this purpose, accurate mechanical properties of cold-formed steels used in the column tests were adopted based on the measured test results of Ranawaka and Mahendran (2009a) and Dolamune Kankanamge and Mahendran (2010). This paper presents the details of the experimental investigation, the results, and a comparison with the predictions of available ambient temperature cold-formed steel design standards and fire design standards, based on which it makes suitable recommendations.

2. Experimental investigation

Suitable test sections and thicknesses were selected based on the standard sections, thicknesses and grades used in structural and architectural applications. Test section dimensions and specimen

lengths were selected based on a series of preliminary analyses using a finite strip analysis program CUFSM and a finite element analysis program ABAQUS so that flexural-torsional buckling governed the test member behaviour at both ambient and elevated temperatures. An electric furnace was designed and built for this research to conduct full scale tests of cold-formed steel columns at elevated temperatures. This furnace consists of three 1000 mm long segments and hence its height can be varied in order to test columns with a height in the range of 500 to 3000 mm.

2.1 Selection of test specimens

Light gauge cold-formed steel thicknesses vary from 0.42 mm to 3 mm and are available in two strength grades, namely high strength (G450, G500 and G550) and low strength (G250 and G300) steels. Therefore three grades (G550, G450 and G250) and thicknesses, G550-0.95 mm, G450-1.90 mm and G250-1.95 mm, were selected to represent the light gauge cold-formed steel domain. The most common cold-formed steel column section of lipped channel section was selected (Fig. 1) and the nominal dimensions of the three selected sections are given in Table 1. It was decided to adopt fixed ends for the tests because perfect pin-end conditions are difficult to create in experiments. Preliminary analyses of lipped channel sections using CUFSM showed that the member lengths of approximately 1600 mm or higher gave flexural-torsional buckling for the selected sections and fixed ends. Therefore specimen lengths of 1800 mm and 2800 mm were chosen in two series of tests.

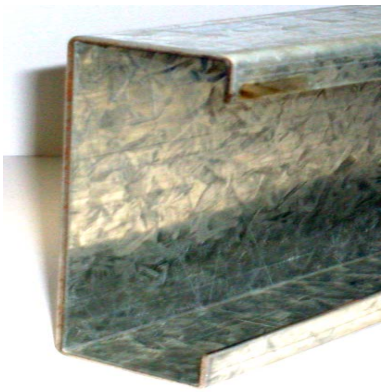

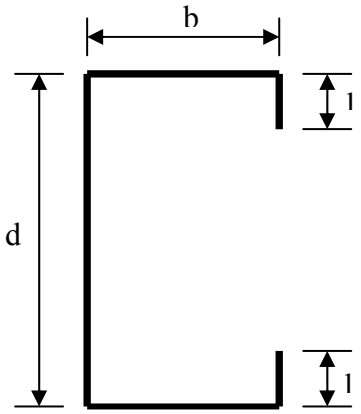

Fig. 1 Lipped channel section

Table 1 Nominal dimensions of lipped channel specimens

Thickness (mm)		Grade	Dimensions (mm)			Length (mm)	
Nominal	Measured		Web	Flange	Lip	Series 1	Series 2
0.95	0.95	550	55	35	9	1800	2800
1.95	1.95	250	75	50	15	1800	2800
1.90	1.88	450	75	50	15	1800	2800

These two series of tests were carried out at ambient and six elevated temperatures up to 700°C (i.e., 20°C, 200 to 700°C at 100°C intervals), giving a total of 39 tests. Test column cross-sections and lengths were selected in order to eliminate local and distortional buckling effects. The selected sections based on CUFSM analyses were further analysed using ABAQUS finite element program to ensure the occurrence of the desired flexural-torsional buckling mode. In both test series, the same cross sections were used (Table 1).

The average base metal thicknesses of cold-formed steels were obtained after removing the coating by immersing them in diluted hydrochloric acid (Table 1). The cross-sectional dimensions and lengths of 39 test columns were measured before the tests (Bandula Heva, 2009) and were used in the analysis of results. Table 2 presents the measured values of yield stress and Young's modulus of steels used to make the test specimens at ambient and elevated temperatures. The reduced mechanical properties of 0.95 mm thick cold-formed steels at elevated temperatures were calculated based on the predictive equations for reduction factors given in Ranawaka and Mahendran (2009a) while those of 1.9 mm and 1.95 mm thick cold-formed steels were taken from Dolamune Kankanamge and Mahendran (2010). The yield stresses were in most cases based on the 0.2% proof stress method due to the absence of a well defined yield point.

2.2. Test set-up and procedure

Since a standard testing machine was not available to test long columns, a special test set-up was designed and built to test long columns of different heights inside the furnace. The test set-up consists of a reaction frame, furnace, control system of the furnace, loading set-up and hydraulic loading system.

2.2.1 Reaction frame

The reaction frame consists of a 2.4 m long 900WB282 cross-head mounted between two 5.0 m high 310UC137 columns (Fig. 2). These two columns were rigidly attached to the strong floor, and were braced in both directions at the top and mid-height.

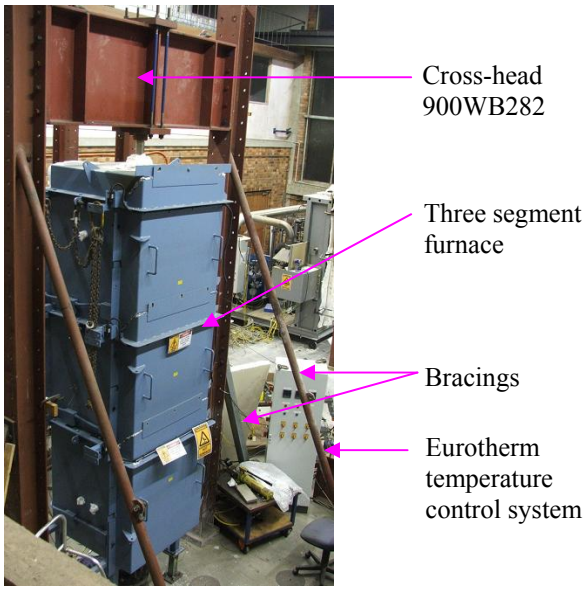

Fig. 2 Three segment furnace and temperature control system

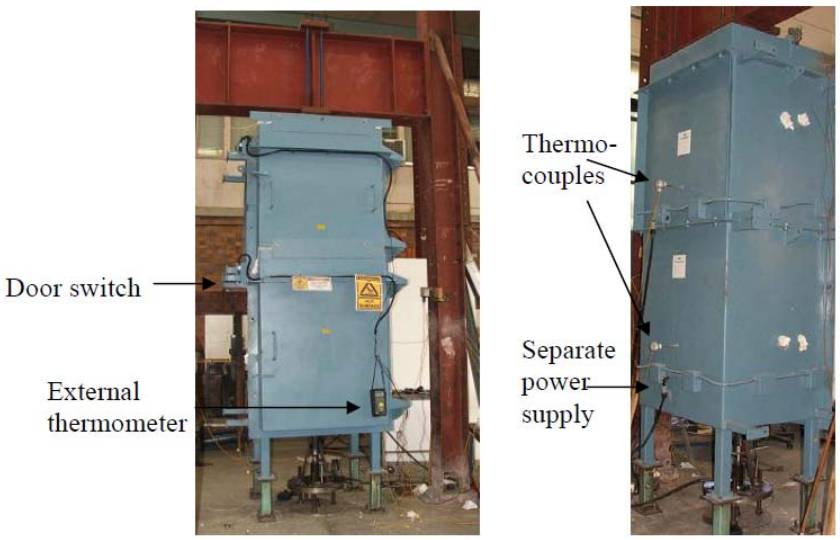

Fig. 3. Two segment furnace

2.2.2 Electric furnace and control system

A new electric furnace was designed to fulfill the requirements of testing cold-formed steel columns of varying heights at different temperatures up to 1000°C. This furnace with three 1 m segments can be assembled as a 3 m, 2 m or 1 m height furnace depending on the specimen height (Figs. 2 and 3). This furnace is heated using the heating coils attached to the inside of their three walls. The heating of each segment can be controlled independently (Fig. 3). Each segment is connected to a Eurotherm control system and has a thermocouple located at the centre of each segment as shown in Fig. 3. Temperature of each segment was monitored by the thermocouple and accordingly Eurotherm controlled the power supply to these segments to maintain the heating rate or target temperature.

2.2.3 Loading arrangement

The loading arrangement consists of two loading shafts at the top and bottom and a hydraulic loading system. The hydraulic loading system consists of a hydraulic pump, a pressure transducer and a hydraulic jack. The parts of top and bottom loading shafts that were located inside the furnace were made with 253MA stainless steel due to their better performance at elevated temperatures up to 1100°C. Loading shafts were made of 70 mm diameter 253MA stainless steel rods to minimise the effects of deformations. The upper loading shaft was inserted through the opening provided in the furnace and then fixed at the top of the furnace (Fig. 4(a)). It was then connected to the cross-head through a 50 mm thick plate attached to the cross-head and tightened using a locknut. The other end of the upper loading shaft located inside the furnace was rigidly fixed to a 150 mm diameter and 25 mm thick 253MA stainless steel plate. This plate was used to fix the specimen to the loading shaft.

At the bottom end, a special loading arrangement was made to fit under the furnace (Fig. 4(b)). A hydraulic jack was used to apply an axial compression load to the specimen. A 70 mm diameter loading shaft and a 150 mm diameter and 25 mm thick plate made of 253MA stainless steel, as used for the upper end, were used at the lower end to fix the specimen.

Table 2 Mechanical properties of steels at ambient and elevated temperatures

Temperature (°C)	0.95mm-G550		1.90mm-G450		1.95mm-G250	
	Yield Stress(MPa)	Young's Modulus (GPa)	Yield Stress (MPa)	Young's Modulus (GPa)	Yield Stress (MPa)	Young's Modulus (GPa)
20	615	205	515	206	271	188
200	596	178	510	175	247	160
300	553	152	489	147	197	134
400	443	125	357	120	143	109
500	276	98	201	92	101	84
600	58	72	57	64	67	58
700	48	45	36	36	37	33

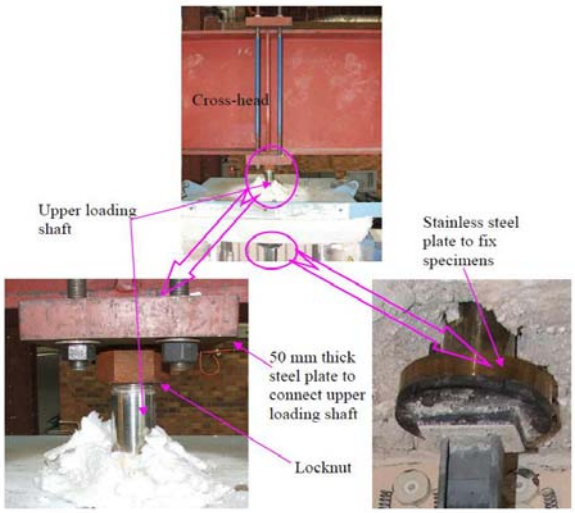

(a)

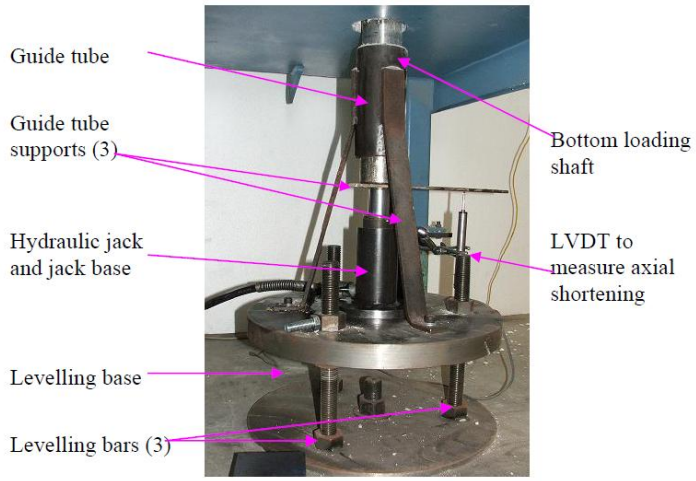

(b)

Fig. 4 Loading Arrangement

The loading shaft was located inside a guide tube which was connected to the levelling base through three additional supports. The levelling base was made of a 40 mm thick and 500 mm diameter circular steel plate to avoid any movement. This levelling base plate was mounted on three 25 mm threaded bars. By screwing the nuts on each of the levelling bars, the base plate was levelled so that the guide tube was vertical. The bottom loading shaft was located on top of the hydraulic jack, which was positioned at the centre of the levelling base. The hydraulic jack was then connected to a hydraulic pump through a pressure transducer. The applied compression load was determined based on pressure transducer measurements.

In the case of compression tests of long columns subject to global buckling, end conditions are very important. The specimen lengths required can be reduced by using pin-ends. Since it was difficult to achieve pure pin-end conditions inside the furnace, all the tests were carried out using fixed-end conditions and longer specimens (1800 mm and 2800 mm). Three segments of the furnace were used for longer columns while two segments were used for shorter columns.

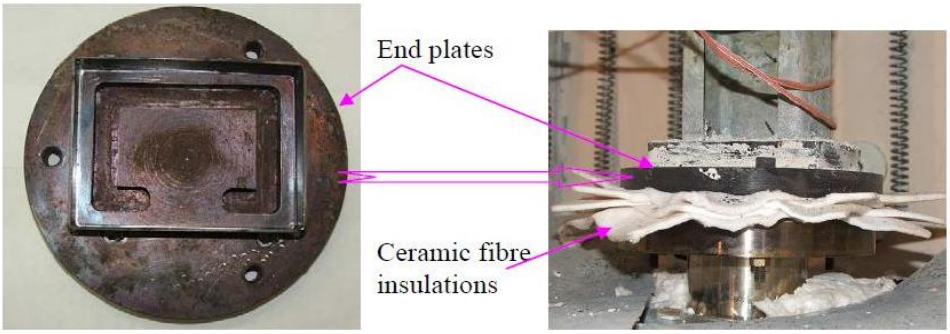

Fig. 5 Details of Fixed End Support

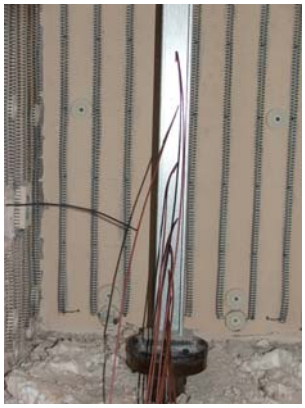

Fig. 6 Measurement of Temperature Profile along the Specimen

To achieve fixed-end supports, special end plates were made to fit the specimen ends (Fig. 5). A groove of 12 mm deep and 10 mm width in the shape of specimen cross-section was made on a 15 mm thick circular steel plate. Geometric centre of the test cross-section was made to coincide with the centre of the plate. A Rectangular Hollow Section (RHS) of 2 mm thick and 15 mm height was then welded to the plate. The specimen was placed within the grove, and 165 procreate coil grout mixed with water was then used to fill the grove and the end space up to the top of RHS. This grout fully hardened within 24 hours.

The specimen with these end plates was then placed between the two loading shafts and bolted to their end plates to form the required fixed end supports. Since steel is a good heat conductor, the heat loss from specimen through the 70 mm diameter loading shafts must be prevented. Therefore ceramic fiber packing was placed between the end plates and the loading shafts for the elevated temperature tests (Fig. 5). This insulation packing reduced the heat loss from test specimens. Due to the heat loss at both ends, it took more time to achieve the uniform target temperatures at the ends of the specimen than in the middle. Therefore thermocouples were attached to both ends of the specimen at closer intervals and the specimen temperature was monitored for tests at higher temperatures (Fig. 6).

All the furnace doors were closed tightly before energizing the power of the furnace. The furnace was then connected to a three phase power supply and temperatures of all the segments were set to the target test temperature. The heating rate to reach the target temperature was about 30ºC/minute. Once the specimen temperature reached the target temperature, the specimen was allowed another 10 minutes before the application of load in order to ensure a uniform temperature in the specimen. During the heating phase, the specimen was allowed to expand when the temperature was increased by maintaining a zero load on the specimen. Once a steady state was reached, the compression load applied to the specimen was increased slowly using the hydraulic jack until failure.

Since it was not possible to employ LVDTs inside the furnace for the purpose of measuring out-of-plane deflections, stainless steel cables were used to connect the specimen to LVDTs located outside the furnace. Ten mm diameter special openings were provided on the furnace at mid-height. Axial shortening was measured using a 50 mm LVDT attached to the bottom loading shaft (Fig. 4 (b)). Ambient temperature tests were also conducted inside the furnace but with doors open.

Initial local and global geometric imperfections of all the test specimens were measured using a measuring table fitted with a laser sensor. Imperfection readings of flange and web elements were taken along the length of the specimens. In most cases, the maximum imperfections were observed to be on the web element and were global type imperfections about the minor axis. The measured global geometric imperfections about the minor axis were significantly less than the tolerance value of L/1000 recommended by AS 4100 (SA, 1998). The mean imperfection values of G550-0.95, G250-1.95 and G450-1.90 specimens of 1800 mm length were L/3437, L/3860 and L/3577 while those of 2800 mm length were L/1406, L/4892 and L/2829, respectively.

3. Test observations and results

In the early stages of the long column test series, test results showed higher capacities than expected for the tests at elevated temperatures. This might have been caused by the temperature distribution along the specimen. Therefore an elevated temperature test was carried out to monitor

At 20°C At 500°C

(a) Failure Mode of Shorter Column Series (1800 mm)

At 20°C At 600°C

(b) Failure Mode of Longer Column Series (2800 mm)

Fig. 7 Flexural-torsional Buckling of G250-1.95 mm Specimens

the temperature profile along the specimen length as shown in Fig. 6. Thermocouples were attached to the specimen at closer intervals along the specimen. The furnace was then set to different elevated temperatures. A considerable temperature difference was observed along the specimen during the heating phase. The difference in the temperature along the specimen length reduced with time. However, this settling time was significantly higher for the target test temperatures of 500°C and above. For the tests below 500°C, the specimen temperature became uniform within a few minutes. Further investigation revealed that 70 mm loading shafts conducted the heat from both ends and thus caused lower temperatures at the ends of the specimen than the middle, particularly at the beginning of the heating phase. Therefore a ceramic fiber insulation packing was placed between the plate on the loading shaft and the end plate of the specimen (Fig. 5). In addition to this, the specimen temperature was monitored, particularly at the ends at closer intervals by attaching thermocouples. Once a uniform temperature was ensured along the specimen length, the load was applied. Affected tests due to the presence of non-uniform temperatures at the ends were repeated, and the repeated test results were used in the numerical studies. As expected, all the test specimens failed by flexural-torsional buckling as shown in Figs. 7 (a) and (b). Since the elevated temperature tests were carried out inside the furnace, the deflected shape could not be observed during the test.

Table 3 Comparison of ultimate loads from tests with code predictions for G250-1.95-2800 test series

Temp. °C	Test (kN)	Test/ Code Prediction				
		DSM	AS/NZS 4600	EC3 Part 1.3	BS 5950 Part 5	EC3 Part 1.2
20	54.07	1.10	1.10	1.29	1.11	1.57
200	48.81	1.15	1.15	1.32	1.16	1.63
300	40.87	1.19	1.19	1.33	1.20	1.71
400	34.70	1.29	1.29	1.39	1.30	1.86
500	29.93	1.50	1.50	1.55	1.51	2.17
600	17.43	1.29	1.29	1.25	1.30	1.86
700	8.20	1.07	1.07	0.95	1.08	1.55
Mean		1.226	1.226	1.298	1.238	1.762
COV		0.121	0.121	0.140	0.148	0.124

Table 4 Comparison of ultimate loads from tests with code predictions for G250-1.95-1800 test series

Temp. °C	Test (kN)	Test/ Code Prediction				
		DSM	AS/NZS 4600	EC3 Part 1.3	BS 5950 Part 5	EC3 Part 1.2
20	87.94	1.15	1.15	1.27	1.08	1.60
200	83.76	1.23	1.23	1.37	1.15	1.72
300	56.07	1.09	1.09	1.17	1.02	1.50
400	45.37	1.18	1.18	1.23	1.11	1.61
500	32.20	1.16	1.16	1.18	1.10	1.57
600	23.03	1.25	1.25	1.25	1.19	1.67
700	12.60	1.21	1.21	1.20	1.15	1.62
Mean		1.183	1.183	1.238	1.117	1.613
COV		0.045	0.045	0.054	0.049	0.071

Table 5 Comparison of ultimate loads from tests with code predictions for G450-1.90-2800 test series

Temp. °C	Test (kN)	Test/ Code Prediction				
		DSM	AS/NZS 4600	EC3 Part 1.3	BS 5950 Part 5	EC3 Part 1.2
20	61.30	1.15	1.15	1.29	1.10	1.36
200	50.64	1.11	1.11	1.20	1.06	1.28
400	43.47	1.40	1.40	1.42	1.33	1.60
500	29.58	1.24	1.24	1.25	1.21	1.51
600	17.16	1.30	1.30	1.27	1.30	1.72
700	9.67	1.22	1.22	1.09	1.23	1.63
Mean		1.237	1.237	1.252	1.205	1.518
COV		0.084	0.084	0.087	0.090	0.112

Table 6 Comparison of ultimate loads from tests with code predictions for G450-1.90-1800 test series

Temp. °C	Test (kN)	Test/ Code Prediction				
		DSM	AS/NZS 4600	EC3 Part 1.3	BS 5950 Part 5	EC3 Part 1.2
20	120.42	1.09	1.12	1.35	1.04	1.45
200	105.99	1.06	1.10	1.30	1.03	1.41
300	83.20	0.95	0.99	1.19	0.93	1.26
400	73.43	1.06	1.11	1.32	1.04	1.42
500	46.35	1.00	1.03	1.16	0.95	1.33
600	17.86	1.03	1.03	1.04	1.00	1.30
700	11.45	1.07	1.07	1.05	1.02	1.36
Mean		1.037	1.062	1.203	1.003	1.363
COV		0.047	0.047	0.104	0.044	0.051

Table 7 Comparison of ultimate loads from tests with code predictions for G550-0.95-2800 test series

Temp. °C	Test (kN)	Test/ Code Prediction				
		DSM	AS/NZS 4600	EC3 Part 1.3	BS 5950 Part 5	EC3 Part 1.2
20	15.85	1.77	1.77	1.82	1.62	1.83
200	12.86	1.65	1.65	1.68	1.50	1.69
400	9.09	1.66	1.66	1.62	1.51	1.69
500	6.34	1.47	1.47	1.40	1.35	1.54
600	4.02	1.29	1.29	1.29	1.36	1.75
700	2.44	1.24	1.24	1.14	1.24	1.55
Mean		1.513	1.512	1.493	1.431	1.674
COV		0.143	0.142	0.174	0.094	0.068

However, the failure pattern of ambient temperature tests was observed because they were conducted with the furnace doors open. The failure pattern of specimens tested at elevated temperatures was determined from the load-deflection curves. Larger deformations, particularly the out-of-plane deflection and twisting, were observed in elevated temperature tests. They were due to the reduced elastic modulii of steel at elevated temperatures and thus lower flexural and torsional rigidities. The observed maximum applied loads are given in Tables 3 to 8 while the measured applied load versus axial shortening and out-of-plane deflection curves are given in Bandula Heva (2009).

Table 8 Comparison of ultimate loads from tests with code predictions for G550-0.95-1800 test series

	Test (kN)	Test/ Code Prediction				
		DSM	AS/NZS 4600	EC3 Part 1.3	BS 5950 Part 5	EC3 Part 1.2
20	24.72	1.17	1.23	1.36	1.13	1.39
200	22.91	1.24	1.31	1.45	1.19	1.45
300	21.33	1.36	1.43	1.57	1.29	1.56
400	20.41	1.58	1.66	1.83	1.50	1.82
600	6.49	1.26	1.27	1.35	1.27	1.88
700	3.50	0.92	0.95	1.14	0.94	1.36
Mean		1.256	1.309	1.451	1.221	1.572
COV		0.174	0.181	0.160	0.154	0.142

4. Comparison of test results with current design standards

Eurocode 3: Part 1.2 (ECS, 2005) provides fire design guidelines for cold-formed steel compression members. Its recommendations were originally developed for Class 1, 2 and 3 sections. However, it recommends the same guidelines for Class 4 sections, which represent cold-formed steel sections. Most importantly, it recommends the use of effective area calculated using ambient temperature mechanical properties for elevated temperature conditions. In addition to this, cold-formed steel design codes, AS/NZS 4600 (SA, 2005), Eurocode 3: Part 1.3 (ECS, 2006), the North American Specification (AISI, 2007), BS 5950 Part 5 (BSI, 1998) and the Direct Strength Method provide design guidelines for compression members at ambient temperature. The North American and Australian/New Zealand specifications provide identical design rules for the prediction of flexural-torsional buckling capacities. Except BS 5950 Part 5, all other design standards give the same equation for the calculation of elastic torsional buckling load. BS 5950 Part 5 includes a factor of two with the warping torsion term in the equation for elastic torsional buckling that gives higher values. The use of this factor also appeared to over-predict the column capacities. Therefore in this study, BS5950 Part 5 predictions are based on the modified equations that are similar to the other design standards. In all the calculations using these design standards the effective length of the specimen was taken as 0.5 times the member length due to the use of fixed ends. Appendix A provides brief details of the design rules in these standards for compression members subject to flexural-torsional buckling.

The new Direct Strength Method (DSM) can be used to predict the member capacity even with the interaction of two or more buckling modes (Schafer, 2001). The DSM formulae are similar to AS/NZS 4600 design rules for flexural and flexural-torsional buckling. However, the DSM uses a different equation (Appendix A) to allow for any occurrence of local buckling with flexural-torsional buckling while AS/NZS 4600 uses an effective area based on the stress corresponding to flexural-torsional buckling (f_n). The difference in the ultimate loads from both methods is insignificant. However, DSM was also considered in this study. In the calculations of member capacities at elevated temperatures using ambient temperature design standards, reduced mechanical properties at elevated temperatures given in Table 2 were used.

All the test ultimate load results are compared with corresponding code predictions at different temperatures in Tables 3 to 8. In most cases the code predictions were found to be conservative. Unexpectedly they were also conservative at ambient temperatures. The test to predicted capacity

ratios were significantly higher at higher temperatures with EC3 Part 1.2 providing the worst comparisons. BS 5950 Part 5, AS/NZS 4600 and DSM provided better comparisons with test results than other codes.

Figs 8 (a) and (b) show the comparison of test results with the AS/NZS 4600 design curve of member capacity ratio N_c/N_s versus member slenderness defined as $\sqrt{\frac{N_y}{N_{cr}}}$ where N_y and N_{cr} are the yield load and the critical elastic buckling load while N_c and N_s are the member and section compression capacities (Appendix A). These Fig.s also show that AS/NZS 4600, NAS and DSM predictions are conservative for both 1800 mm and 2800 mm long columns. Their predictions for high strength steel columns are more conservative than those for low strength steel columns. For long columns, the ultimate compression loads are sometimes higher than their elastic buckling loads. This is more dominant for higher strength steel columns. Since AS/NZS 4600 and DSM limit the column capacity to 87.7% of the elastic buckling load, the code predictions were found to be very conservative, particularly for long columns made of high strength steels as seen in Figs. 8 (a) and (b).

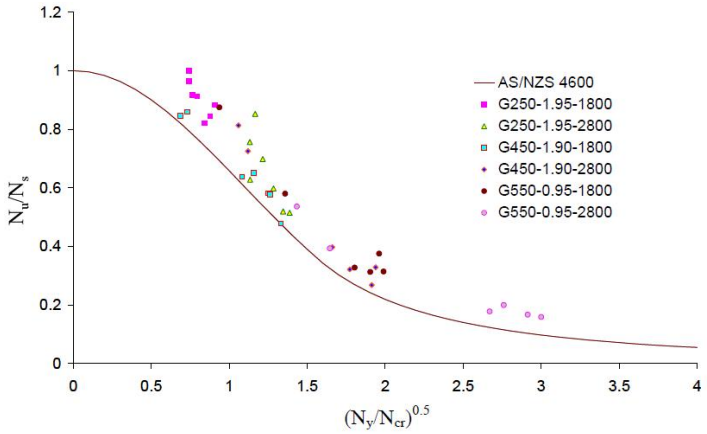

(a) Based on length and grade of steel

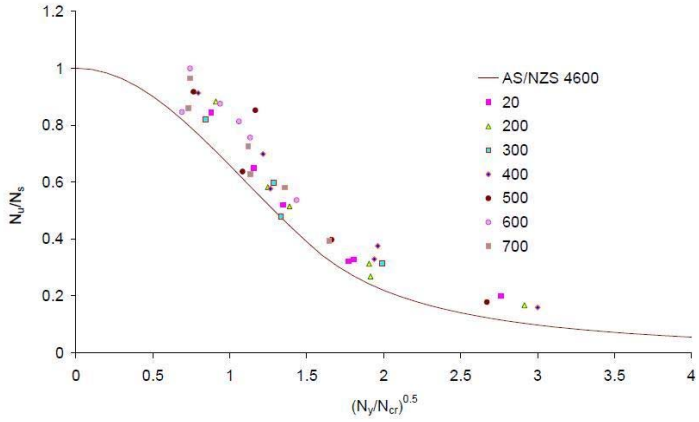

(b) Based on temperature

Fig. 8 Comparison of test results with AS/NZS 4600 design curve

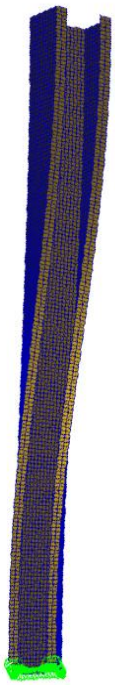

Fig. 9. Flexural-torsional Buckling of G450-1.9-1800 Column from FEA

4.1 Ambient temperature tests

This research was focused on developing suitable design methods for cold-formed steel columns subject to flexural-torsional buckling at elevated temperatures based on the ambient temperature design rules. Ambient temperature tests were expected to confirm the adequacy of the current design rules in predicting the column capacities. However, test results in Tables 3 to 8 and Figs. 8 (a) and (b) show that the current ambient temperature design rules are conservative.

Finite element analyses (FEA) of the tested columns were also undertaken using a shell finite element model with measured dimensions and mechanical properties (Bandula Heva, 2009). Elastic buckling and nonlinear analyses of half-length column models confirmed the occurrence of flexural-torsional buckling of all the tested columns (Fig. 9). The measured overall imperfections were used in the nonlinear analyses. The FEA ultimate loads of all the columns at ambient temperature agreed well with corresponding test ultimate loads with a difference of less than 5% (Table 9). Except for G550-0.95-2800 columns, FEA ultimate loads were slightly higher than the test ultimate loads. Hence both FEA and test results confirm that the current ambient temperature design rules are conservative for cold-formed steel columns subject to flexural-torsional buckling. Possible reasons are discussed next.

All the design rules for compression members are based on a nominal imperfection of L/1000. However, the measured geometric imperfections of tested columns were significantly lower than L/1000. Therefore the test ultimate loads could be higher than the code predictions. In order to determine the effect of imperfections, finite element analyses of test columns with an increased imperfection of L/1000 were undertaken using the same model developed in Bandula Heva (2009)

at ambient temperature. However, the ultimate load results indicated that the difference in ultimate loads is less than 2% for the test columns.

AS/NZS 4600 and DSM based design rules limit the flexural-torsional buckling capacity of slender columns to 87.7% of the elastic buckling load. This is one of the reasons for the lower ultimate loads predicted by AS/NZS 4600 and DSM. Chen and Young (2007a) also showed that these design rules are conservative for high strength cold-formed steel columns. Their finite element analyses of three series of lipped channel columns made of G450 steels showed that the predicted ultimate loads from these design rules are always less than the FEA ultimate loads for the slender columns with lengths of 2, 2.5 and 3 m. The ratio of ultimate loads from FEA and design rules was in the range of 1.05 to 1.40. These observations confirm that AS/NZS 4600 and DSM design rules for flexural-torsional buckling are conservative for cold-formed steel columns at ambient temperature.

EC3 Part 1.3 design rules are based on the buckling curve 'b' (imperfection factor α of 0.34) for cold-formed lipped channel sections. Their predicted loads are lower than the test ultimate loads as seen in Tables 3 to 8. The use of the buckling curve based on "a_0" will improve the accuracy of their predictions. In comparison to other design codes, EC3 Part 1.2 predictions are more conservative for cold-formed steel columns at ambient temperature. This is due to the use of a higher imperfection factor α (>0.34) as a result of using an equation based on yield stress (Eq.21 in Appendix A). The imperfection factors for G250-1.95, G450-1.90 and G550-0.95 steel columns from this equation are 0.61, 0.44 and 0.40, respectively. Hence all the ambient temperature design curves based on EC3 Part 1.2 are below the EC3 Part 1.3 curve (Fig.10), and thus lead to very conservative predictions. Unlike the predictions of other design standards, EC3 Part 1.2 predictions for low strength steel columns are of the same order as high strength steel columns because of the conservative design curve for lower yield stresses.

Further research is currently under way to determine the reasons for the conservative predictions of the ambient temperature design standards. Finite element analyses of cold-formed sections made of varying geometry, steel thicknesses and grade, and member lengths are being used for this purpose.

4.2 *Elevated temperature tests*

Fig. 8 (b) and Tables 3 to 8 show the comparison of test results with code predictions for varying elevated temperatures. Comparison of results at ambient temperature has shown that the ambient temperature design rules are conservative.

Table 9 Comparison of ultimate loads of columns at ambient temperature from tests and FEA

Column Section	Ultimate Load (kN)		Ult. Load Test/FEA
	Test	FEA	
G250-1.95-1800	87.94	90.70	0.970
G450-1.90-1800	120.42	129.00	0.933
G550-0.95-1800	24.72	25.40	0.973
G250-1.95-2800	54.07	56.30	0.960
G450-1.90-2800	61.30	63.80	0.961
G550-0.95-2800	15.85	15.40	1.029

Hence as expected the use of the same rules with appropriately reduced mechanical properties at elevated temperatures also produced conservative predictions in most cases. All the design rules used in this study led to higher test to predicted load ratio with increasing temperatures up to about 500-600°C, followed by an improvement in prediction at 700°C. Similar variations were seen in Chen and Young's (2007a) FEA results of high strength slender cold-formed steel columns at uniform elevated temperatures.

This higher conservatism observed for temperatures in the range of 200-600°C may be due to the following reasons. In the elevated temperature tests beyond 400°C, the temperature at the ends was slightly less than the temperature in the middle of the specimen. As explained in Section 3, such possible non-uniform temperature distributions along the specimens in the tests reported in this paper were minimized through the use of ceramic fibre insulations at the ends and by monitoring the specimen temperatures using thermocouples. Finite element analyses also showed that the ultimate loads of slender columns are not affected unless the level of non-uniformity of temperature distribution along the specimen is increased considerably. Hence it is considered that the effect of non-uniform temperature distributions along the specimen length on the ultimate load is minimal for the tests reported in this paper.

The comparison of test results with code predictions for varying temperatures identifies another important reason that explains the differences in results apart from those discussed already in this paper. The comparisons show the presence of larger differences at higher temperatures of 300°C and above. This is likely to be due to the non-linear stress-strain characteristics of steels at elevated temperatures (Ranawaka and Mahendran, 2009a, Dolamune Kankanamge and Mahendran, 2010). It was found that the limit of proportionality is about 50 to 75% of the yield stress for G250 and G450 steels at 300 to 700°C. Such significant levels of non-linearity in material stress-strain characteristics will influence the ultimate column capacities at elevated temperatures. The differences in the levels of nonlinearity with temperature and steel grade are one of the reasons for the scatter in the results in Fig. 8 (b). However, the capacity predictions using the current design rules were based on the yield stresses determined using the 0.2% proof stress method (Table 2), and hence would have contributed to the increased differences in results.

Among the ambient temperature design standards, the modified BS 5950 Part 5 design rules provide more accurate results while EC3 Part 1.3 design rules predict more conservative results. EC3 Part 1.3 recommends the use of buckling curve "b" for channel sections. Since its predictions are too conservative, it appears that the buckling curve 'b" is not suitable for channel sections. The buckling curves "a" or "a_o" with reduced imperfection factors (α) are likely to predict more accurate capacities than buckling curve "b".

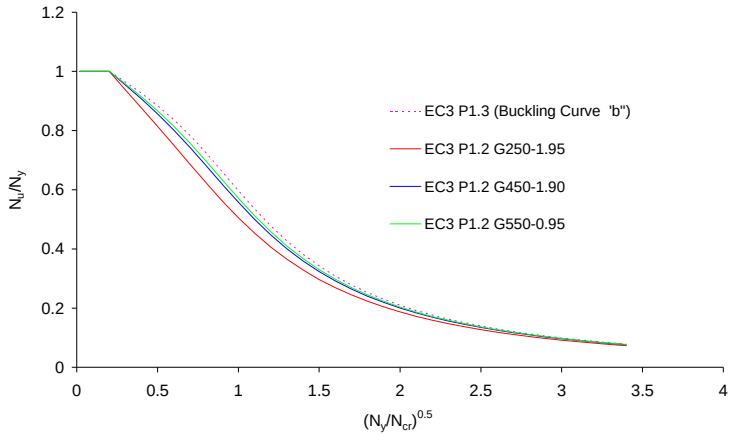

Fig. 10 Design Curves of Eurocode 3 Parts 1.2 and 1.3

Based on these discussions, it can be concluded that BS 5950 Part 5, AS/NZS 4600 and the DSM based design rules and EC3 Part 1.3 with a suitable buckling curve ('a' or 'a_o) can be used safely to predict the flexural-torsional buckling capacities of cold-formed steel columns at elevated temperatures by simply using the reduced mechanical properties of steels. In order to improve the accuracy of these design rules further for elevated temperature conditions, their accuracy should be first established for ambient temperature conditions. The accuracy of EC3 Part 1.3 design rules can be improved for cold-formed steel columns by the choice of a suitable buckling curve (a or a_0). The accuracy of AS/NZS 4600 and DSM design rules can also be further improved by suitable modifications to the current design rules (Eqs.2, 3, 24 and 25). Such modifications can also include the removal of the factor 0.877 in Eqs.3 and 25. However, further research is needed using cold-formed sections made of other geometries, steel thicknesses and grades, and member lengths that were not considered in this paper. Following this, the effects of non-linear stress-strain characteristics of steels at elevated temperatures must be included in these ambient temperature design rules to enable an improved and uniform accuracy at all the elevated temperatures. Detailed numerical studies are currently being undertaken for this purpose.

The predictions of the fire design standard, EC3 Part 1.2, are overly conservative and are greater than those predicted by the ambient temperature design standards as shown in Fig. 10. Hence EC3 Part 1.2 predictions are more conservative than EC3 Part 1.3 predictions at ambient and elevated temperatures. Therefore it appears that EC3 Part 1.2 design rules are unsuitable for the design of cold-formed steel compression members subject to flexural-torsional buckling.

5. Conclusions

Flexural-torsional buckling behaviour and strength of cold-formed steel compression members were investigated using 39 full scale tests at ambient and elevated temperatures. Three cold-formed steel thicknesses and grades, G550-0.95 mm, G450-1.9 mm and G250-1.95 mm, were selected to represent light gauge cold-formed steels. The most commonly used section type of lipped channel section was selected with two lengths, 1800 mm and 2800 mm, so that flexural-torsional buckling occurred in the tests. Experimental ultimate load results were compared with the predictions from different cold-formed steel design standards, which showed that ambient

temperature design standard guidelines can be safely used to predict the flexural-torsional buckling capacities at elevated temperatures when appropriately reduced mechanical properties are used. However, they appear to be conservative at ambient and elevated temperatures. Based on the experimental results and comparisons reported here, this paper has made suitable conclusions regarding the accuracy of flexural-torsional buckling rules in a number of ambient temperature cold-formed steel standards and suggested methods of possible improvement. The accuracy of the relevant design rules in the fire design standard, Eurocode 3 Part 1.2, was also reviewed and it was found to give overly conservative predictions than the ambient temperature design standards. This paper has also presented valuable experimental results for slender cold-formed steel columns at elevated temperatures.

References

American Iron and Steel Institute (AISI) (2007), North American Specification for the Design of Cold-formed Steel Structural Members, AISI, Washington, DC, USA.

Ali, F. and O'Connor, D. (2001), "Structural performance of rotationally restrained steel columns in fire," *Fire Safety J.*, **36**(7), 679-691.

Bandula Heva, Y. (2009) Behaviour and Design of Cold-formed Steel Compression Members at Elevated Temperatures, PhD Thesis, QUT, Brisbane, Australia.

British Standards Institution (BSI) (1998), British Standard 5950: Structural Use of Steelwork in Buildings, Part 5: Code of Practice for Design of Cold-formed Thin Gauge Sections, London, UK.

British Standards Institution (BSI) (2005), British Standard 5950: Structural Use of Steelwork in Buildings, Part 8: Code of Practice for Fire Resistant Design, London, UK.

Burgrees, I.W., Olawale, A.O. and Plank, R.J. (1992), "Failure of steel columns in fire", *Fire Safety J.*, **18**(2), 183-201.

Chen, J. and Young, B. (2007a), "Cold-formed steel lipped channel columns at elevated temperatures, *Eng. Struct*.", **29**(10), 2445-2456.

Chen, J. and Young, B. (2007b), "Experimental investigation of cold-formed steel material at Elevated temperatures", *Thin-Walled Struct*., **45**(1), 96-110.

Dolamune Kankanamge, N. and Mahendran, M. (2010). "Mechanical properties of cold-formed steels at elevated temperatures", *Thin-Walled Struct*., **49**(1), 26-44.

European Committee for Standardization (ECS) (2005) Eurocode 3 EN 1993-1-2, Design of Steel Structures, General Rules, Structural Fire Design, Brussels, Belgium.

European Committee for Standardization (ECS) (2006) Eurocode 3 EN 1993-1-3 Design of Steel Structures, General rules - Supplementary rules for Cold-formed Thin Gauge Members and Sheeting, Brussels, Belgium.

Feng, M., Wang, Y. C. and Davies J. M. (2003a), "Structural behaviour of cold-formed thin-walled short steel channel columns at elevated temperatures, Part 1: Experiments", *Thin-Walled Struct*., **41**(6), 543-570.

Feng, M., Wang, Y.C. and Davies, J.M. (2003b), "Structural behaviour of cold-formed thin-walled short steel channel columns at elevated temperatures. Part 2: Design calculations and numerical analysis", *Thin-Walled Struct.,* **41**(6), 571-594.

Feng, M., Wang, Y.C. and Davies, J.M. (2003c), "Axial strength of cold-formed thin-walled steel channels under non-uniform temperatures in fire," *Fire Safety J*., **38**(8), 679-707.

Feng, M., Wang, Y.C. and Davies, J.M. (2004), "A numerical imperfection sensitivity study of cold-formed thin-walled tabular steel columns at uniform elevated temperatures", *Thin-Walled Struct*., **42**(4), 533-555.

Franssen, J.M., Cooke, G.M.E. and Latham, D.J. (1995), "Numerical simulation of a full scale fire test on a loaded steel framework", *J. of Constr. Steel Res*., **35**(3), 377-408.

Franssen, J.M., Schleich, J.B., Cajot G.L. and Azpaizu, W. (1996), "A simple model for the fire resistance of axially loaded members compression with experimental results", *J. of Constr. Steel Res.,* **37**(3), 175-204.

Ranawaka, T. and Mahendran, M. (2009a), "Experimental study of the mechanical properties of light gauge cold-formed steels at elevated temperatures", *Fire Safety J*., **44**(2), 219-229.
Ranawaka, T. and Mahendran, M. (2009b), "Distortional buckling tests of cold-formed steel compression members at elevated temperatures", *J. of Constr. Steel res*., **65**(2), 249-259.
Ranawaka, T. and Mahendran, M. (2009c), "Numerical modelling of light gauge cold-formed steel compression members subjected to distortional buckling at elevated temperatures", *Thin-Walled Struct*., **48**(4-5), 334-344.
Ranby, A. (1998) "Structural fire design of thin-walled steel sections", J. of Constr. Steel Res.", **46**(1-3), 303-304.
Standards Australia (SA) (2005) Australian/New Zealand Standard, AS/NZS 4600:2005, Cold-formed Steel Structures, Sydney, Australia.
Schafer, B.W. (2001), Thin-walled Column Design Considering Local, Distortional and Euler Buckling, Proceedings of the Structural Stability Research Council Annual Stability Conference, Ft. Lauderdale, FL, USA, 419-438.
Talamona, D., Franssen, J.M., Schleich, J.B., and Kruppa, J. (1997), "Stability of steel columns in case of fire: Numerical modelling", *J. of Struct. Eng*., **123**(6), 713-720.
Wang, Y.C. and Davies, J.M. (2003a), "Fire tests of non-sway loaded and rotationally restrained steel column assemblies", *J. of Constr. Steel Res*., **59**(3), 359-383.
Wang, Y.C. and Davies, J.M. (2003b), "An experimental study of non-sway loaded and rotationally restrained steel column assemblies under fire conditions: Analysis of test results and design calculations", *J. of Constr. Steel Res*., **59**(3), 291-313.
Yang, K.C., Lee, H.H. and Chen, O. (2006), "Performance of Steel H Columns Loaded under Uniform Temperature", *J. of Constr. Steel Res*., **62**(3), 262-270.

CC

Appendix A. Design rules for cold-formed steel columns subject to flexural-torsional buckling

AS/NZS 4600 (SA, 2005) and NAS (AISI, 2007)

AS/NZS 4600 (SA, 2005) gives the flexural or flexural-torsional buckling capacity (N_c) based on the non-dimensional slenderness of the column (λ_c) as given next.

$$N_c = A_e f_n \tag{1}$$

$$f_n = \left(0.658^{\lambda_c^2}\right) f_y \quad \lambda_c \le 1.5 \tag{2}$$

$$f_n = \left(0.877 \Big/ \lambda_c^2\right) f_y \quad \lambda_c > 1.5 \tag{3}$$

where

$$\lambda_c = \sqrt{\frac{f_y}{f_{cr}}} \tag{4}$$

A_e = Effective area of section calculated based on f_n to allow for local buckling effects
f_y = yield stress
f_{cr} = least of the elastic flexural buckling stress (f_{ox}), torsional (f_{oz}) and flexural-torsional buckling stress (f_{oxz})

$$f_{ox} = \frac{\pi^2 E}{\left(l_{ex}/r_x\right)^2} \tag{5}$$

$$f_{oz} = \frac{GJ}{Ar_{oi}^2}\left(1 + \frac{\pi^2 EI_w}{GJl_{ez}^2}\right) \tag{6}$$

$$f_{oxz} = \frac{1}{2\beta}\left[\left(f_{ox} + f_{oz}\right) - \sqrt{\left(\left(f_{ox} + f_{oz}\right)^2 - 4\beta f_{ox} f_{oz}\right)}\right] \tag{7}$$

where, l_{ex} and l_{ez} = effective lengths about x (symmetry axis) and z axes
r_x = radius of gyration of the full, unreduced cross-section

$$\beta = 1 - \left(x_o/r_{ol}\right)^2 \tag{8}$$

r_{ol} = Polar radius of gyration about the shear centre
x_o = Distance between shear centre and geometric centre
E, G = Young's modulus and Shear modulus
A, J, I_w = Section properties: Gross area, Torsion & Warping constants

This paper uses the same symbols for the common parameters in the following codes.

BS 5950 Part 5 (BSI, 1998)

BS 5950 Part 5 (BSI, 1998) calculations are based on loads instead of stresses. The flexural buckling capacity P_c is given next where the critical elastic buckling load P_{Ecr} is taken as the minimum value of elastic flexural buckling load (P_{Ex} or P_{Ey}) and the elastic flexural torsional buckling load P_{TF} . Elastic buckling load equations are identical to those of AS/NZS 4600 except in the case of elastic torsional buckling load (P_T) where a factor of 2 is used with the warping component.

$$P_c = \frac{P_{Ecr} P_{cs}}{\varphi + \sqrt{\varphi^2 - P_{EM} P_{cs}}} \tag{9}$$

$$\phi = \frac{P_{cs} + (1+\eta) P_E}{2} \tag{10}$$

Local buckling capacity

$$P_{CS} = A_e f_y \tag{11}$$

L_e / r is the slenderness ratio about the critical axis,
For

$$L_e / r \le 20, \quad \eta = 0 \tag{12a}$$

For

$$L_e / r > 20, \quad \eta = 0.002(\alpha L_e / r - 20) \tag{12b}$$

$$\alpha = \sqrt{\frac{P_E}{P_{TF}}} \tag{13}$$

where P_E is the minimum elastic flexural buckling load.

Eurocode 3 Part 1.3 (ECS, 2006)

Eurocode 3 Part 1.3 (ECS, 2006) provides the following equation for flexural-torsional buckling resistance $(N_{b,Rd})$.

$$N_{b,Rd} = \chi \beta_A A f_y \tag{14}$$

$$\chi = \frac{1}{\phi + \left(\phi^2 - \bar{\lambda}^2 \right)^{0.5}} \quad \text{but} \quad \chi \le 1.0 \tag{15}$$

$$\phi = 0.5 \left[1 + \alpha \left(\bar{\lambda} - 0.2 \right) + \bar{\lambda}^2 \right] \tag{16}$$

α is an imperfection factor depending on the appropriate buckling curve = 0.34 for C-sections

(Curve '*b*'), and the relative slenderness is defined as follows.

$$\overline{\lambda} = \sqrt{\left(f_y / f_{cr}\right)}\sqrt{\beta_A} \tag{17}$$

with $f_{cr} = f_{oxz}$, but $f_{cr} \le f_{oz}$ and $\beta_A = A_e / A$

Eurocode 3 Part 1.2 (ECS, 2005)

The design buckling resistance $N_{b,fi,t,Rd}$ at time t and temperature θ of a compression member can be calculated from Eq. (18). Effect of local buckling is included by using the effective area (A_e) calculated at ambient temperature.

$$N_{b,fi,t,Rd} = \chi_{fi} A k_{y,\theta} f_y \tag{18}$$

where χ_{fi} is the reduction factor for flexural buckling in a fire design situation;

The value of χ_{fi} should be taken as the lesser of the values about *x* and *y* axes.

$$\chi_{fi} = \frac{1}{\varphi_\theta + \sqrt{\varphi_\theta^2 - \overline{\lambda}_\theta^2}} \tag{19}$$

$$\varphi_\theta = \frac{1}{2}\left[1 + \alpha\overline{\lambda}_\theta + \overline{\lambda}_\theta^2\right] \tag{20}$$

Imperfection factor

$$\alpha = \beta\sqrt{235/f_y} \tag{21}$$

β is the severity factor used to provide an appropriate safety level = 0.65.

The non-dimensional slenderness $\overline{\lambda}_\theta$ for the temperature θ_a is given by:

$$\overline{\lambda}_\theta = \overline{\lambda}\left[k_{y,\theta} / k_{E,\theta}\right]^{0.5} \tag{22}$$

where $\overline{\lambda}$ is the relative slenderness at ambient temperature and is defined in Eq. (17).

$k_{E,\theta}$ and $k_{y,\theta}$ are the reduction factors for E and f_y at temperature θ_a reached at time t.

Direct Strength Method

Member capacity allowing for local buckling effects is given by

$$N_{cl} = \left[1 - 0.15\left(\frac{N_{ol}}{N_{ce}}\right)^{0.4}\right]\left(\frac{N_{ol}}{N_{ce}}\right)^{0.4} N_{ce} \quad \text{for} \quad \lambda_l > 0.776, \tag{23a}$$

Else

$$N_{cl} = N_{ce} \tag{23b}$$

$$N_{ce} = \left(0.658^{\lambda_c^2}\right) N_y \quad \lambda_c \leq 1.5 \tag{24}$$

$$N_{ce} = \left(0.877 \Big/ \lambda_c^2\right) N_y \quad \lambda_c > 1.5 \tag{25}$$

where

N_{ol} = Elastic local buckling load of the section.

λ_l = non-dimensional slenderness used to determine

$$N_{cl} = \sqrt{\frac{N_{ce}}{N_{ol}}} \tag{26}$$

λ_c = non-dimensional slenderness used to determine

$$N_{ce} = \sqrt{\frac{N_y}{N_{cr}}} \tag{27}$$

N_{cr} = least of the elastic compression member buckling load in flexural, torsional or flexural-torsional buckling

N_y = nominal yield capacity of the of the member in compression